

Vascular healing after kissing balloon inflation: Nine-month 3D optical coherence tomography analysis in corelab

Masahiro Yamawaki^{a,*}, Takayuki Okamura^b, Ryoji Nagoshi^c, Tatsuhiro Fujimura^b, Yoshinobu Murasato^d, Shiro Ono^e, Takeshi Serikawa^f, Yutaka Hikichi^g, Hiroaki Norita^h, Fumiaki Nakaoⁱ, Tomohiro Sakamoto^j, Toshiro Shinke^k, Junya Shite^c

^a Department of Cardiology, Saiseikai Yokohama City Eastern Hospital, Japan

^b Department of Medicine and Clinical Science, Yamaguchi University Graduate School of Medicine, Japan

^c Department of Cardiology, Osaka Saiseikai Nakatsu Hospital, Japan

^d Department of Cardiology, National Hospital Organization Kyusyu Medical Center, Japan

^e Department of Cardiology, Saiseikai Yamaguchi General Hospital, Japan

^f Department of Cardiology, Fukuoka Wajiro Hospital, Japan

^g Department of Cardiovascular Medicine, Saga Medical Center KOSEIKAN, Japan

^h Department of Cardiology, Oda Hospital, Japan

ⁱ Department of Cardiology, Yamaguchi Grand Medical Center, Japan

^j Department of Cardiology, Saiseikai Kumamoto General Hospital, Japan

^k Department of Cardiology, Showa University Graduate School of Medicine, Japan

ARTICLE INFO

Keywords:

Percutaneous coronary intervention
Coronary bifurcation lesions
Kissing balloon technique
Optical coherence tomography
Drug eluting stent

ABSTRACT

Background: The jailing strut configuration with link-free and distal guidewire recrossing (LFD) at the side branch orifice (SBO) reduces incomplete stent apposition (ISA) after kissing balloon technique (KBT) in crossover stenting of coronary bifurcation lesions (CBLs). However, data regarding vascular healing after KBT are lacking. We investigated vascular healing 9 months after crossover stenting followed by KBT with optical coherence tomography (OCT) guidance in a prospective multicenter registry.

Methods: Fifty-nine patients with CBLs (LFD, 35 patients; non-LFD, 24 patients) were studied. The jailing configuration of the SB and the wire-recrossing position, incidence of ISA and uncovered struts, and neointima unevenness score (NUS) in the main vessel (MV) after 9 months were determined by off-line 3D-OCT in the core laboratory.

Results: The ISA rate was significantly higher at the SB ostium and distal MV after KBT in the non-LFD group, compared to the LFD group. After 9 months, incidence of ISA (18.3 ± 18.2 vs. $6.0 \pm 8.7\%$, $p < 0.01$) and uncovered struts (8.7 ± 9.9 vs. $4.7 \pm 7.3\%$, $p = 0.08$) were higher at the SB ostium with higher SB restenosis in the non-LFD group. In distal MV, NUS was significantly higher (3.1 ± 1.1 vs. 2.5 ± 0.6 , $p < 0.05$). In true-CBLs, an increase in uncovered struts and ISA rate was prominent in the proximal MV and opposite SB. No differences were observed in the 9-month clinical outcomes.

Conclusion: Visualization of the wire recrossing point and the SB-jailing strut pattern by OCT plays an important role to optimize the KBT in CBL stenting, resulting in favorable mid-term vascular healing.

Abbreviations: PCI, Percutaneous coronary intervention; OCT, optical coherence tomography; LFD, link-free and distal guidewire recrossing; SB, side branch; MV, main vessel; ISA, incomplete stent apposition; KBT, kissing balloon technique; CBLs, coronary bifurcation lesions; NUS, neointima unevenness score; POT, proximal optimization technique; LA, lumen area; SA, stent area; NIA, neointima area; NIT, neointima thickness; SEI, stent eccentricity index; QCA, quantitative coronary angiographic analysis; DS, diameter stenosis; MSA, Minimum stent area; WSS, wall shear stress; MEI, minimum expansion index; SBO, side branch orifice.

* Corresponding author at: Division of Cardiology, Saiseikai Yokohama City Eastern Hospital, 3-6-1 Shimosueyoshi Tsurumi-ku, Yokohama, Japan.

E-mail address: m.yamawaki@tobu.saiseikai.or.jp (M. Yamawaki).

<https://doi.org/10.1016/j.ijcha.2022.101034>

Received 22 January 2022; Received in revised form 12 March 2022; Accepted 14 April 2022

2352-9067/© 2022 Published by Elsevier B.V. This is an open access article under the CC BY-NC-ND license (<http://creativecommons.org/licenses/by-nc-nd/4.0/>).

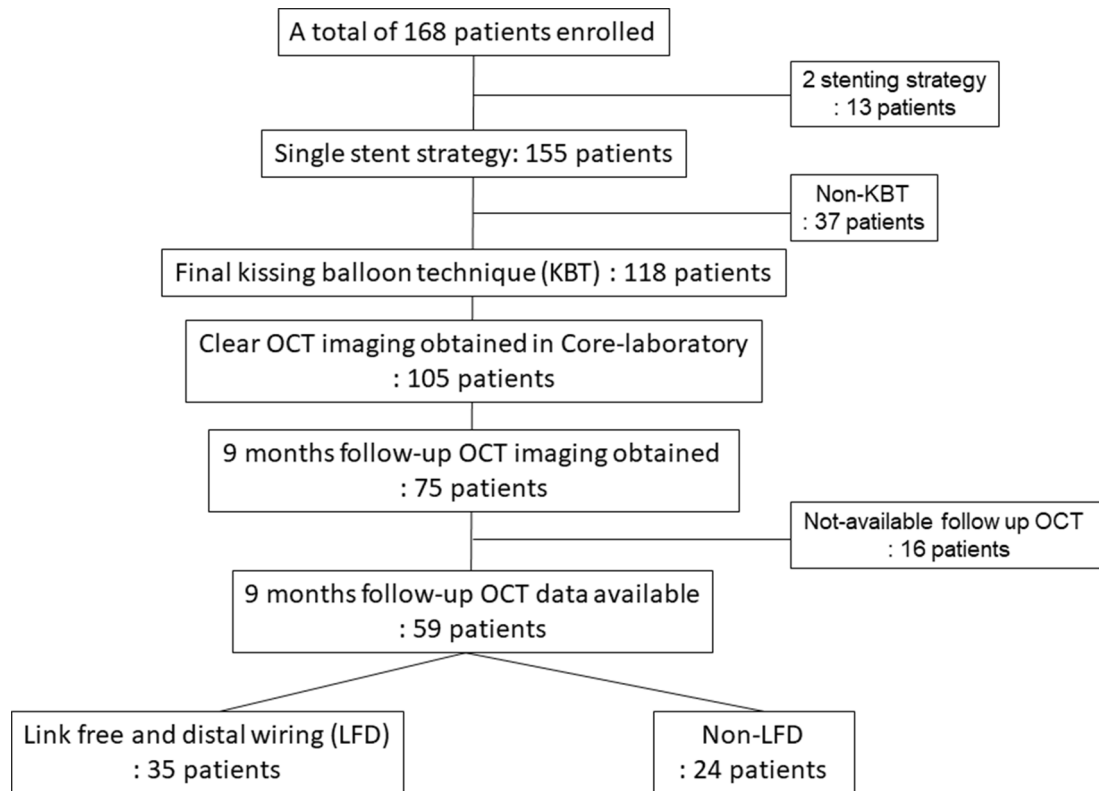


Fig. 1. Patients flow chart. OCT = optical coherence tomography.

1. Introduction

Coronary bifurcation lesions (CBLs) represent 15–20% of all percutaneous coronary interventions (PCIs) [1]. In the treatment of CBLs, stent requires modification of the cylindrical geometry to fit the nature tapering anatomy of the CBL [2]. This modification includes proximal optimization technique (POT), standard post dilatation, isolated short balloon SB angioplasty, and kissing balloon technique (KBT) [3].

Under current guidelines, the provisional single-stent strategy is the default stenting technique [4]. After crossover drug-eluting stenting (DES), wire recrossing to the jailed side branch (SB) near the carina is recommended before KBT to remove metal struts at the SB ostium and to reconstruct the natural shape and restore rheology at CBLs [2]. PROPOT randomized trial, which compared KBT and POT followed by SB angioplasty in a provisional single-stent strategy, showed no difference in the rate of strut malapposition or in that of SB-jailing struts [5]. Angiography is inherently limited in the visualization of both the carina and the stent structure to achieve an appropriate wire recrossing point [2]. A recent randomized clinical trial evaluating angiography and 3-dimensional optical frequency domain imaging (3D-OFDI) guided PCI for CBLs demonstrated the superiority of 3D-OFDI guided PCI in terms of the reduction of acute incomplete stent apposition (ISA) rate [2]. We reported the association between the location of the link and wire recrossing position after crossover stenting before KBT and ISA rate using the provisional single-stent strategy [6]. It was found that link-free and distal wiring (LFD) was related to the reduction of ISA immediately after KBT [6]. However, there are no data concerning the effect of ISA on vascular healing after KBT. The main objective of the present study was

to investigate the influence of wire-recrossing point and stent link location on 9-month vascular healing assessed by follow-up optical coherence tomography (OCT) imaging.

2. Methods

2.1. Study design

The 3D-OCT bifurcation registry is a multicenter prospective registry that enrolled patients with de novo CBLs with SBs with a diameter of at least 2 mm treated with OCT-guided PCI in 10 participating hospitals from June 2014 to December 2015. Inclusion and exclusion criteria, procedure and OCT acquisition were shown in a previous article [6]. Based on the Helsinki Declaration in 1975, the study protocol was approved by the medical ethics committee at all institutions. Informed consent was obtained from all individual participants included in the study.

2.2. 3D OCT reconstruction and angiographic analysis in core-laboratory

In this follow-up OCT study, details of wire recrossing position and jailing configuration in the 3D-OCT bifurcation registry were used [6]. Briefly, the link-connecting type had a link to the carina, while the link-free type had no link to the carina [6]. The larger area enclosed by both the carina and the stent strut, with at least one distal top of the stent hoop located on the SB ostium, was defined as the *distal cell*. The small triangular area enclosed by the most distal hoop and the carina was defined as the *far distal cell*, which was included into the distal rewiring

Table 1
Patient and lesion characteristics.

	LFD (n = 35)	Non-LFD (n = 24)	p-value
Male	27 (77)	16 (67)	0.37
Age	69 ± 10	73 ± 7	0.07
Hypertension	30 (86)	22 (92)	0.94
Dyslipidemia	29 (83)	16 (67)	0.15
Diabetes mellitus	16 (46)	11 (46)	0.99
Current smoking	21 (60)	12 (50)	0.45
Target vessel			
Left main coronary artery	14 (40)	8 (33)	
Left anterior descending artery	16 (46)	10 (42)	0.59
Right coronary artery	3 (9)	2 (8)	
Left circumflex artery	2 (6)	4 (17)	
Medina bifurcation class			
(0–0–1)	1 (3)	2 (8)	
(0–1–0)	7 (20)	13 (54)	
(0–1–1)	4 (11)	4 (17)	0.05
(1–0–0)	2 (6)	1 (4)	
(1–0–1)	5 (14)	1 (4)	
(1–1–0)	6 (17)	2 (8)	
(1–1–1)	10 (29)	1 (4)	
True bifurcation lesion	19 (54)	6 (25)	<0.05
Quantitative coronary angiography			
Proximal main vessel			
Reference diameter, mm	3.0 ± 0.5	3.2 ± 0.8	0.33
Diameter stenosis			
Before, %	31.2 ± 23.9	22.4 ± 27.6	0.21
After, %	8.7 ± 9.2	3.9 ± 5.8	<0.05
Distal main vessel			
Reference diameter, mm	2.4 ± 0.5	2.5 ± 0.7	0.76
Diameter stenosis			
Before, %	41.5 ± 19.6	48.9 ± 21.8	0.15
After, %	10.8 ± 8.8	13.9 ± 10.3	0.24
Side branch			
Reference diameter, mm	2.3 ± 0.5	2.4 ± 0.7	0.54
Diameter stenosis			
Before, %	28.4 ± 22.6	25.5 ± 18.5	0.62
After, %	21.0 ± 14.4	30.0 ± 17.1	<0.05
Lesion length in MV, mm	22.7 ± 11.4	23.8 ± 11.9	0.77
Lesion length in SB, mm	12.1 ± 7.4	10.0 ± 5.9	0.36
Angle, proximal and distal MV, °	153.2 ± 19.5	158.2 ± 18.0	0.39
Angle, proximal MV - SB, °	147.0 ± 22.6	141.6 ± 18.2	0.35
Angle, distal MV - SB, °	59.3 ± 24.0	60.1 ± 16.5	0.89

N(%), LFD = link-free on carina and distal guidewire recrossing, MV = main vessel, SB = side branch.

in this study [6]. In the present study, patients were divided into two groups depending on the jailing configuration and rewiring position as follows: *LFD group* with both link-free (LF) type and distal (D) guidewire recrossing; and the *non-LFD group* which included all other cases [6]. The inter- and intra-observer agreement on the rewiring position were 0.9093 and 0.8638, respectively.

Frame-by-frame cross-sectional images were analyzed on each frame at the bifurcation segment and at 1-mm intervals 5-mm proximal and distal to the bifurcation. ISA was defined when the distance between the strut marker and the lumen contour was greater than the specific strut thickness plus the axial resolution of the OCT (14 μm) [6]. The lumen area (LA), stent area (SA), neointima area (NIA), and neointima thickness (NIT) were measured. The NIA was calculated as SA minus LA. The same definition was applied for ISA, non-apposed SB struts, and uncovered struts at four segments: (1) the proximal MV (extending 5-mm proximal to the first cross-section where the SB was visible), (2) two sides of bifurcation (divided into two 180° halves toward or opposite the ostium of the SB), and (3) distal MV (extending 5-mm from the last cross-section in which the SB was visible) [6]. To assess stent asymmetry

Table 2
Procedure characteristics.

	LFD (n = 35)	Non-LFD (n = 24)	p-value
Implanted stent type			
Xience	7 (20)	8 (33)	
Ultimaster	3 (9)	1 (4)	0.69
Nobori	8 (23)	5 (21)	
Resolute	11 (31)	8 (33)	
Promus	6 (17)	2 (8)	
3-link platform DES	7 (20)	8 (33)	0.25
Stent size in main vessel	3.0 ± 0.4	3.0 ± 0.5	0.82
Stent length in main vessel	24.0 ± 7.0	24.0 ± 7.4	0.84
Proximal optimization technique	16 (46)	7 (29)	0.20
POT balloon diameter	3.5 ± 0.3	3.5 ± 1.0	0.99
Recross wire attempt for side branch			
–1	27 (77)	19 (79)	
–2	7 (20)	4 (17)	0.92
–≥3	1 (3)	1 (4)	
Reclosing in distal cell	35 (100)	16 (67)	<0.01
Link free to carina	35 (100)	2 (8)	<0.01
KBT balloon diameter in MV	3.1 ± 0.4	3.0 ± 0.6	0.60
KBT balloon pressure in MV	9.9 ± 3.4	9.1 ± 2.3	0.34
KBT balloon diameter in SB	2.3 ± 0.4	2.3 ± 0.5	0.80
KBT balloon pressure in SB	8.1 ± 3.0	8.4 ± 2.5	0.34
Bailout stent for SB	0 (0)	1 (4)	0.41
Re-POT	7 (20)	4 (17)	0.91
Contrast amount, ml	149 ± 50	159 ± 48	0.39
Radiation time	39 ± 21	30 ± 14	0.05

DES = drug eluting stent, KBT = kissing balloon technique, LFD = link-free on carina and distal guidewire recrossing, MV = main vessel, POT = proximal optimization technique, SB = side branch.

expansion, the average stent eccentricity index (SEI) was determined by dividing the minimum stent diameter by the maximum stent diameter in the proximal and distal MV. We also evaluated the neointima unevenness score (NUS) to assess uneven neointimal distribution within the proximal and distal MVs. NUS was calculated using a previously reported method [7,8]. Neointima tissue type was defined as a homogeneous and heterogeneous pattern. For quantitative coronary angiographic analysis (QCA), bifurcation-dedicated tools (QAngio XA version 7.3, Medis Specials, Leiden, the Netherlands) was used.

2.3. Clinical outcome

Nine-month clinical follow-up data were obtained from all patients. Cardiac death, myocardial infarction (MI), target lesion revascularization (TLR, defined as repeated PCI or coronary artery bypass grafting to the target lesion), stent thrombosis (Academic Research Consortium definitions), and the composite end points of major adverse cardiovascular events (MACE, defined as cardiac death, MI, TLR, and stent thrombosis) were evaluated.

2.4. Statistical analysis

The results are expressed as the mean ± standard deviation for continuous variables and as percentages for categorical data. We performed the Pearson bivariate analysis, chi-square test, and Fisher's exact test for categorical analysis between the groups. An unpaired *t*-test, Mann-Whitney *U* test, analysis of variance with post-hoc Tukey's test, and Kruskal-Wallis test were used for continuous variables.

Inter- and intra-observer agreement for assessment of jailing configuration was assessed by the kappa statistic. Statistical significance was set at $p < 0.05$. The analyses were performed using the SPSS

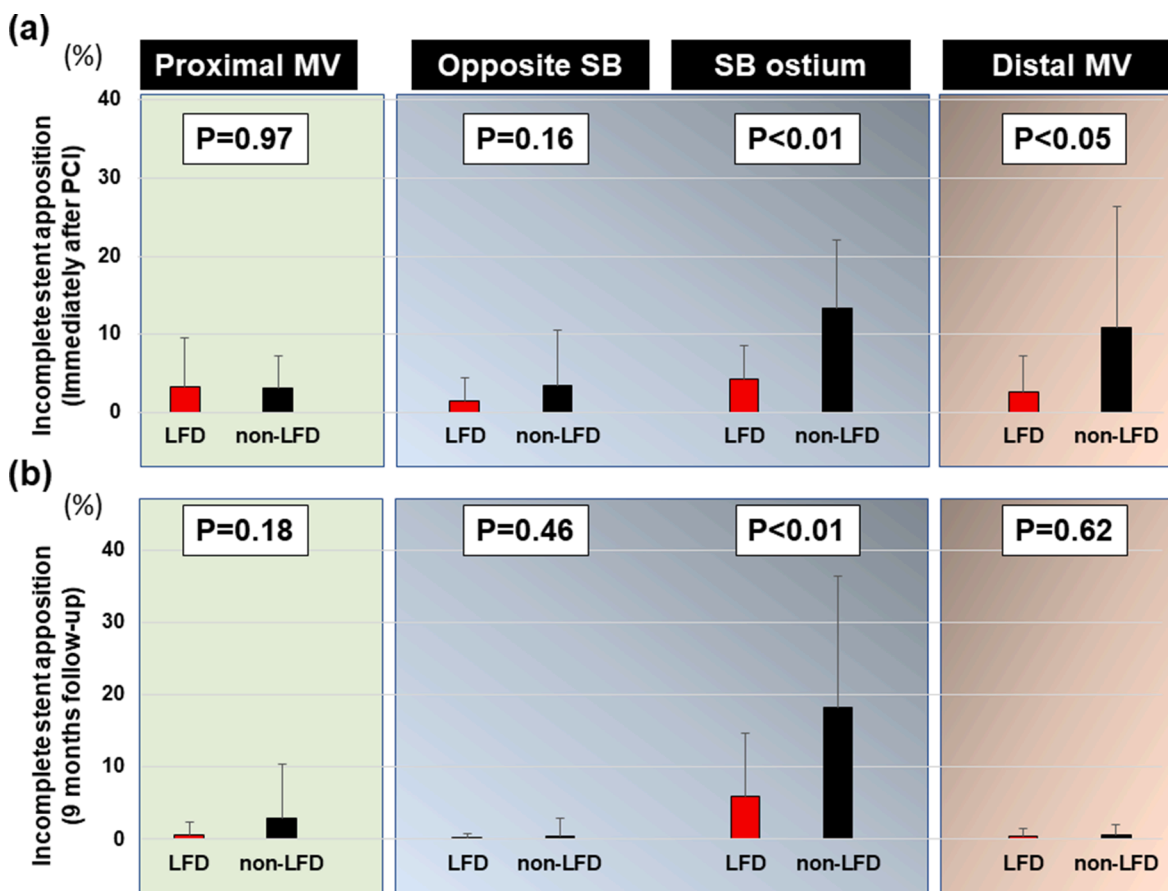


Fig. 2. ISA rate immediately after PCI (a) and ISA rate 9 months after PCI (b) in each segment such as proximal MV (light green box on left), opposite SB and SB ostium (light gray box in center), and distal MV (beige box on right). Red bars indicate LFD group, and black bars display non-LFD group. PCI = percutaneous coronary intervention, ISA = incomplete stent apposition, MV = main vessel, SB = side branch, LFD = link-free type and distal guidewire recrossing. (For interpretation of the references to colour in this figure legend, the reader is referred to the web version of this article.)

software (version 21.0, SPSS Chicago, IL, USA).

3. Results

3.1. Patient, lesion, and procedure characteristics

The patient flowchart is shown in Fig. 1. Patient and lesion characteristics and pre-/post-procedure QCA are shown in Table 1. Regarding lesion characteristics, true-CBLs were less frequently observed in the non-LFD group than in the LFD group (25% vs. 54%, $p < 0.05$). Procedure characteristics is displayed in Table 2.

The rate of link free to carina immediately after crossover stenting (8 vs. 100%, $p < 0.01$) or recrossing in the distal cell to the SBs (67 vs. 100%, $p < 0.01$) was significantly lower in the non-LFD group. Radiation time was numerically shorter in the non-LFD group (30 ± 14 vs. 39 ± 21 min, $p = 0.05$).

In QCA, immediately after PCI, % diameter stenosis (DS) at SB was larger in non-LFD- than LFD group (30.0 ± 17.1 vs. 21.0 ± 14.4 mm, $p < 0.05$) and smaller in proximal MV (3.9 ± 5.8 vs. 8.7 ± 9.2 %, $p < 0.05$), respectively (Table 1).

3.2. OCT analysis in core-laboratory

Immediately after the procedure, the incidence of ISA was

Table 3
Nine-month OCT analysis.

	LFD (n = 35)	Non-LFD (n = 24)	p-value
Incident of thrombus	4 (11)	3 (13)	0.60
Proximal MV			
Average stent area, mm ²	8.1 ± 2.7	8.5 ± 3.5	0.67
Average neointima area, mm ²	0.6 ± 0.6	0.4 ± 0.6	0.17
Average neointima thickness, μ m	95.4 ± 55.6	71.0 ± 34.0	0.07
Average lumen area, mm ²	7.5 ± 2.7	8.1 ± 3.7	0.49
Neointima type: hetero	4 (11)	3 (13)	0.60
Bifurcation segment			
Neointima type: hetero	4 (11)	4 (16)	0.42
Distal MV			
Average stent area, mm ²	6.2 ± 1.7	6.3 ± 2.2	0.94
Average neointima area, mm ²	0.6 ± 0.7	0.5 ± 0.4	0.48
Average neointima thickness, μ m	107.5 ± 58.2	88.8 ± 49.3	0.21
Average lumen area, mm ²	5.6 ± 1.7	5.7 ± 2.3	0.77
Neointima type: hetero	5 (14)	2 (8)	0.40

LFD = link-free on carina and distal guidewire recrossing, MV = main vessel, OCT = Optical coherence tomography.

significantly higher in the non-LFD group than in the LFD group at the SB ostium (13.4 ± 8.6 vs. 4.2 ± 4.4 %, $p < 0.01$) as well as in the distal MV (10.9 ± 15.5 vs. 2.6 ± 4.6 %, $p < 0.05$) (Fig. 2a). The ISA rate

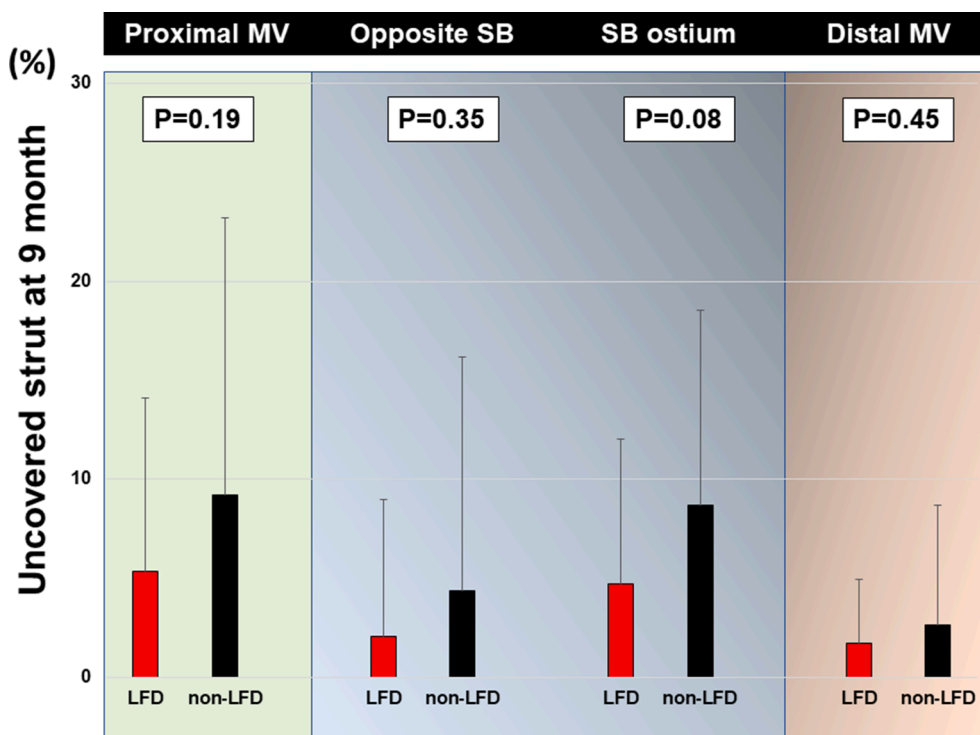


Fig. 3. The incidence of uncovered strut at 9 months in each segment such as proximal MV (light green box on left), opposite SB and SB ostium (light gray box in center), and distal MV (beige box on right). Red bars indicate LFD group, and black bars display non-LFD group. Same abbreviations are used as Fig. 2. (For interpretation of the references to colour in this figure legend, the reader is referred to the web version of this article.)

tended to be higher at opposite of SB (3.4 ± 7.1 vs. 1.4 ± 3.2 %, $p = 0.16$). Average SEI was similar between non-LFD- and LFD group in proximal MV (0.85 ± 0.07 vs. 0.86 ± 0.07 , $p = 0.61$), and tended to be higher in distal MV (0.90 ± 0.04 vs. 0.87 ± 0.06 , $p = 0.06$). Minimum stent area (MSA) immediately after PCI was significantly smaller in the distal MV than in the proximal MV (5.6 ± 1.9 vs. 7.5 ± 2.7 mm², $p < 0.001$). Lesions with MSA < 4.5 mm² were more frequently observed in the distal MV than in the proximal MV (33 % vs. 9 %, $p < 0.01$).

Nine-month OCT data are shown in Table 3. Actual follow-up durations was 309 ± 46 days in non-LFD group and 310 ± 31 days in LFD group ($p = 0.95$). No difference was observed between the two groups regarding average SA, NA, NIT, and LA, as well as the incidence of thrombus and type of neointima proliferation.

Fig. 2b illustrates the incidence of ISA at 9 months. ISA rate was numerically higher in non-LFD than LFD group in proximal MV (2.8 ± 7.6 vs. 0.7 ± 1.8 %, $p = 0.18$), and significantly higher at SB ostium (18.3 ± 18.2 vs. 6.0 ± 8.7 %, $p < 0.01$, Fig. 2b). The incidence of uncovered struts at 9 months is shown in Fig. 3. Uncovered strut rates were numerically higher in the proximal MV (9.2 ± 14.0 vs. 5.4 ± 8.7 %, $p = 0.19$) and at the SB ostium (8.7 ± 9.9 vs. 4.7 ± 7.3 %, $p = 0.08$). NUS, demonstrated in Fig. 4, was significantly higher in the distal MV (3.1 ± 1.1 vs. 2.5 ± 0.6 , $p < 0.05$). Fig. 5 displays representative cases of LFD (5A) and non-LFD (5B and 5C). Figs. 6, 7 and Fig. 8 represents the sub-analysis by true-CBLs. After PCI in patients with non-true-CBLs, ISA rate was higher in non-LFD than LFD group at SB ostium (right part in light gray box in Fig. 6a) and distal MV (beige box in Fig. 6a). This difference was significantly pronounced in those with true-CBLs (SB ostium: 15.8

± 11.5 vs. 4.3 ± 3.9 %, $p < 0.01$; distal MV: 19.9 ± 22.1 vs. 2.6 ± 3.8 %, $p < 0.01$, Fig. 6a). In true-CBLs, ISA rate at opposite of SB was significantly higher in non-LFD group (9.2 ± 12.9 vs. 1.5 ± 2.8 , $p < 0.05$, left part in light gray box in Fig. 6a). The ISA rate after 9 months is shown in Fig. 6b. In true-CBLs, the higher incidence of ISA is still observed in the non-LFD group both at opposite SB (1.9 ± 4.8 vs. 0.04 ± 1.2 %, $p < 0.05$, left part of light gray box in Fig. 6b) and ostial SB (28.1 ± 24.1 vs. 5.6 ± 7.3 %, $p < 0.01$, right part of light gray box in Fig. 6b). Regarding uncovered strut rates after 9 months (Fig. 7), non-LFD in true-CBLs was numerically greater in proximal MV ($p = 0.06$, light green box in Fig. 7), and significantly higher in the opposite of SB ($p < 0.01$, left part of light gray box in Fig. 7). NUS in the distal MV was significantly higher in the non-LFD group than in the LFD group ($p < 0.05$, beige box in Fig. 8).

3.3. Clinical and angiographic outcome in 9 months

SB restenosis was numerically higher in the non-LFD group than in the LFD-group (25% vs. 6%, $p = 0.08$); however, no statistically significant differences in MACE were observed between the two groups (Table 4). A sub-analysis of %DS comparing LFD- and non-LFD groups by true-CBLs is shown in Table 5. No difference was observed in MV. For SB, immediately after and 9 months after PCI, %DS in non-LFD with true-CBLs was significantly higher than that in other conditions ($p < 0.05$).

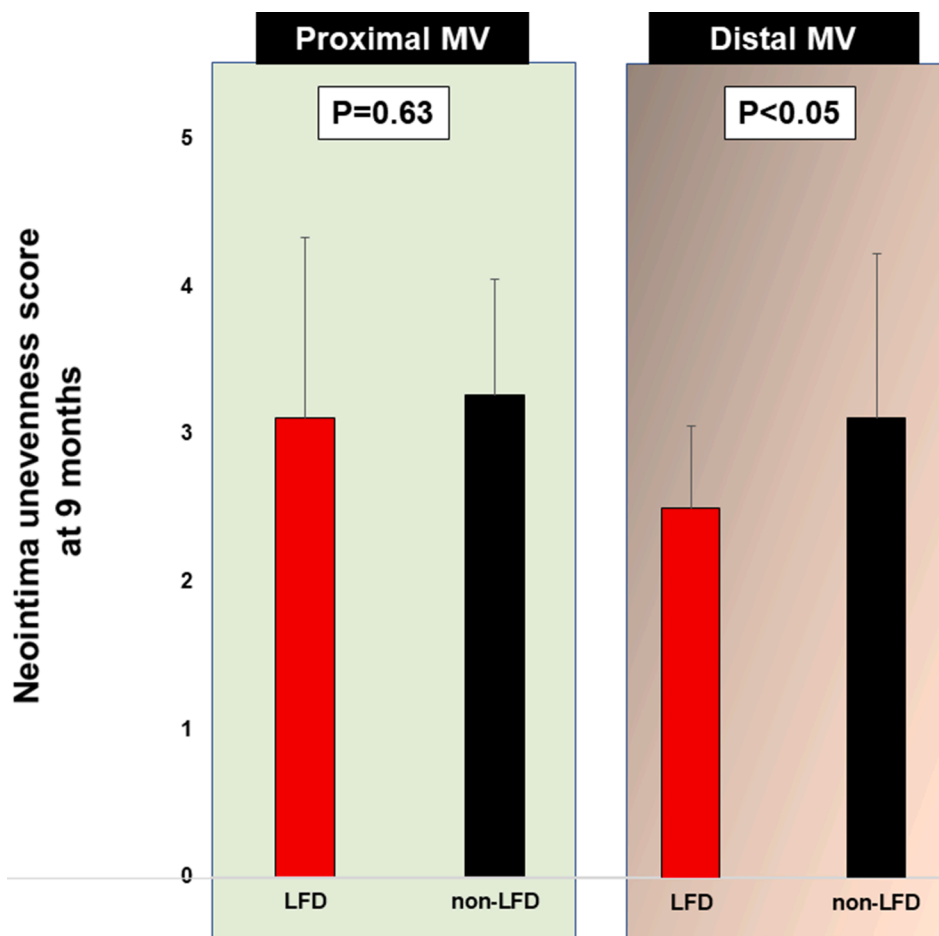


Fig. 4. (a) Neointima unevenness score at 9 months in each segment such as proximal MV (light green box on left), SB (light gray box in center) and distal MV (beige box on right). NUS was not analyzed due to lack of SB strut opened by KBT in bifurcation core segment, (For interpretation of the references to colour in this figure legend, the reader is referred to the web version of this article.)

4. Discussion

The present study is the first to evaluate the influence of wire-recrossing point to jailed SB on 9-month vascular healing, as assessed by OCT, in patients undergoing single crossover stenting with final KBT.

Our data indicated the following points in non-LFD, compared with LFD: (1) ISA rate was significantly higher at the SB ostium and distal MV immediately after KBT (2) after 9 months, the incidence of ISA and uncovered struts was higher in SB with a numerically higher rate of SB restenosis, and (3) uneven neointima proliferation was observed in distal MV.

4.1. Midterm result in SB

After 9 months, the ISA rate remained significantly higher at the SB ostium in the non-LFD group. In true-CBLs, this trend was obvious at the ostial SB, and uncovered struts were more frequently observed at the opposite of SB in the non-LFD group. Furthermore, non-LFD patients with true-CBLs displayed a higher %DS at SB.

Neointimal coverage was delayed in the malapposed strut at the SB orifice. Uncovered struts have been recognized as risk factors for thrombosis formation after DES implantation [7]. The coexistence of high and low wall shear stress (WSS) and an increase in its oscillation behind the SB-jailed strut might activate platelet deposition, thrombus formation, and neointimal proliferation [9]. A recent OCT study revealed that thrombus formation in SB-jailed and floating struts in the bifurcation core, and the degree of intimal coverage of the SB-jailed strut depended on the performance of the final KBT [10]. Despite these accumulated data, the clinical benefit of SB opening by KBT after crossover single stenting has been debated [11,12].

The operator cannot completely control the link position in front of the SB orifice. Our registry data suggested a potential limitation of routine performance of KBT in terms of complete elimination of ISA, uncovered strut, and uneven neointimal proliferation after 9 months. However, 3D-OCT-guidance might be an effective modality to confirm the avoidance of proximal wire-recrossing. Furthermore, in complex true CBLs, appropriate lesion modification to avoid carina shift and optimal POT might create a workspace for optimal re-wiring to SB

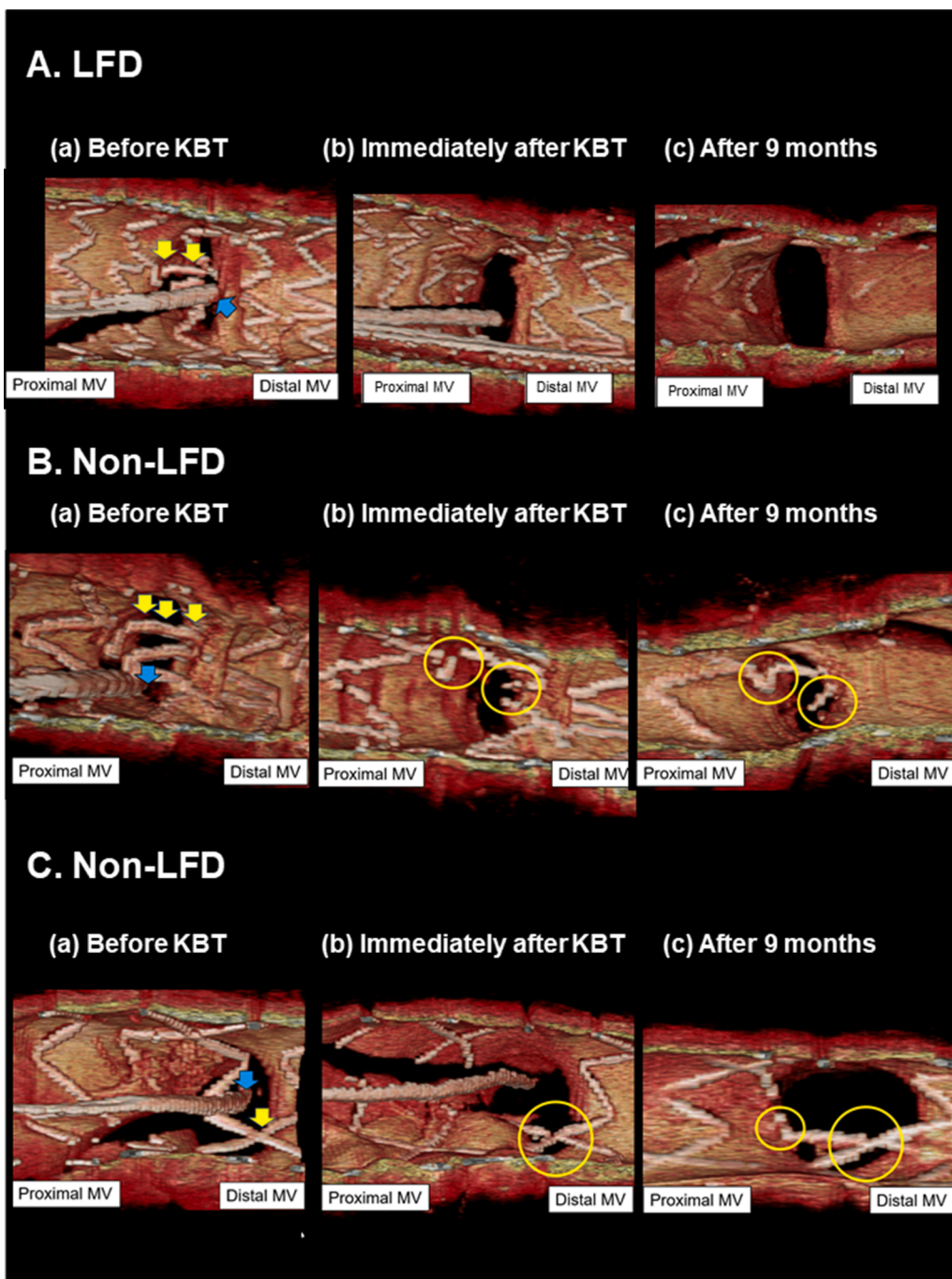


Fig. 5. Representative cases in LFD group (A) and non-LFD group (B) (C). (a) Before KBT, link connecting crowns was not located (A) and located on carina (B)(C) (yellow arrows). The guide-wire was inserted in distal cell of crossover stent (blue arrows). (b) Immediately after KBT, struts at SB orifice were completely removed, and stent apposition was optimally achieved (A). However, in case (B) and (C), strut removal was incomplete, and ISA was observed at both the proximal MV and SB ostium (B) and at the SB ostium (C) (yellow circle). (c) After 9 months, neo-intimal coverage was well observed (A), whereas not well observed, and ISA remained in the proximal MV and SB orifice (B) (C) (yellow circle). Same abbreviations are used as Fig. 2. KBT = kissing balloon technique. (For interpretation of the references to colour in this figure legend, the reader is referred to the web version of this article.)

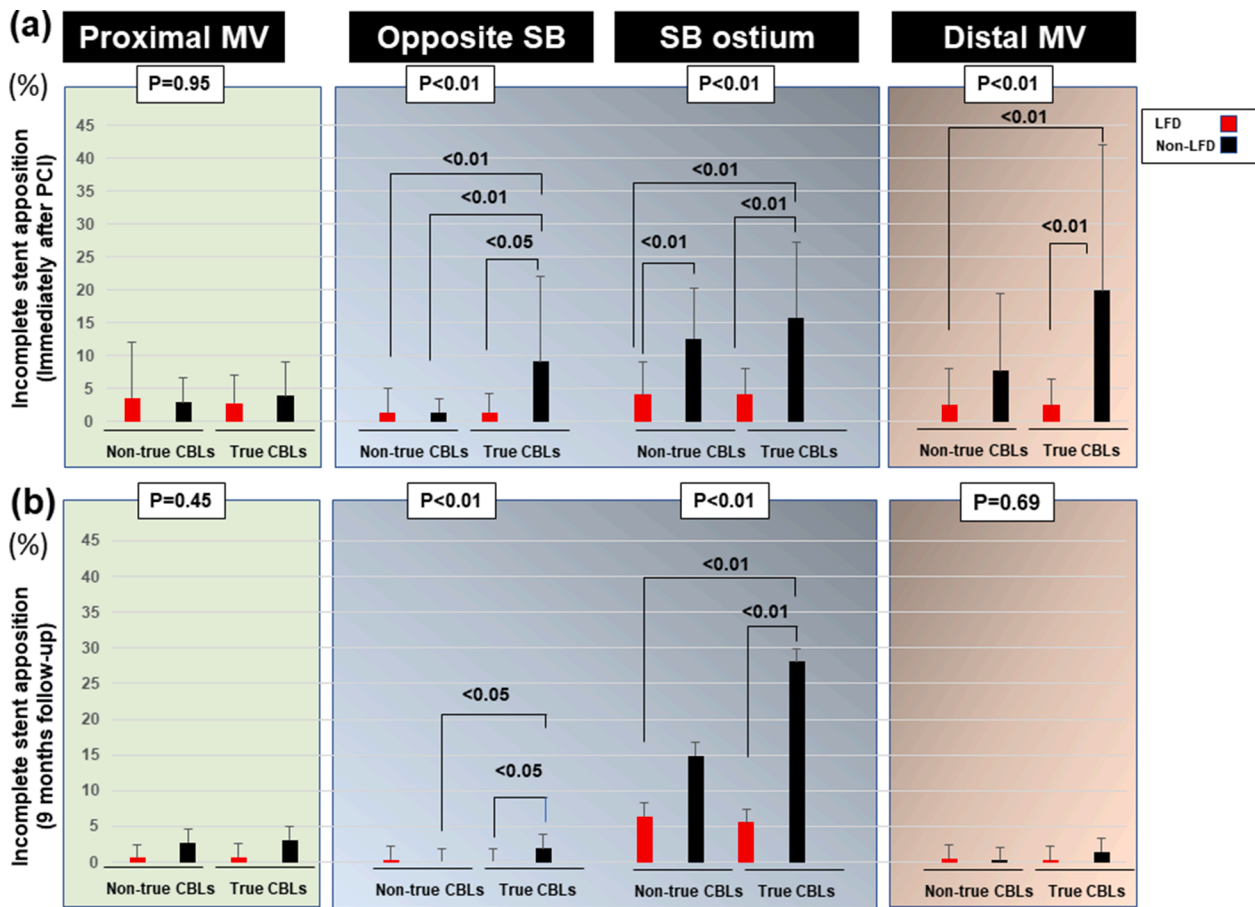


Fig. 6. ISA rate immediately after PCI (a) and ISA 9 months after PCI (b) in proximal MV (light green box on left), opposite SB and SB ostium (light gray box in center), and distal MV (beige box on right) by true CBLs. Red bars indicate LFD group, and black bars display non-LFD group. CBLs = coronary bifurcation lesions. Same abbreviations are used as Fig. 2. (For interpretation of the references to colour in this figure legend, the reader is referred to the web version of this article.)

[13,14]. Despite these techniques, when the most distal stent link is in contact with the rim of the carina, consensus report on the use of OCT in CBLs by European and Japanese Bifurcation Club recommended that a second distal compartment is considered as the optimal cell, and in the presence of multiple second distal compartment, the larger compartment should be selected [15]. Otherwise, a novel balloon push-fold method that removes jailed SB struts may be an option when the guidewire crosses the proximal cell [16]. OCT optimization of complex bifurcation for routine use or ad-hoc evaluation of selected patients dependent on the results of ongoing Optical Coherence Tomography Optimized Bifurcation Event Reduction Trial (OCTOBER) [17].

4.2. Midterm result in MV

In the present study, non-LFD was associated with a numerically higher incidence of ISA and uncovered struts in proximal MV and significantly uneven neointimal proliferation in distal MV after 9 months.

We speculated that, in the non-LFD condition, the SB KBT balloon might not effectively scaffold the strut on the vessel wall between the

proximal MV (the side of the SB) and the SB ostium because of the deformation connected with the stent link and the potential existence of plaque and calcification in true-CBLs. As a result, although the acute result of ISA rate was comparable, stent strut might not be effectively embedded in the plaque, and the vascular response of neointimal proliferation might be moderate after 9 months.

In the distal MV, the acute ISA rate was higher in the non-LFD group. Interestingly, ISA was comparable to the coverage of neointima proliferation after 9 months. However, in the non-LFD group, uneven neointimal growth was observed. After bifurcation stenting in the MV, local flow hemodynamics occurred with low WSS in the lateral wall and high WSS in the carina [18]. Low WSS facilitates the migration of smooth muscle progenitor cells from the bone marrow to the stented site, leading to the acceleration of neointimal growth [18]. This mechanism might explain the comparable ISA rate in distal MV after 9 months. A previous OCT study investigating vascular response 6 months after DES implantation indicated that thrombus formation was associated with a smaller SEI and greater NUS [7]. Neointima proliferation was inversely correlated with SEI, which was explained by uneven drug delivery to the vessel wall induced by ISA and asymmetric stent expansion [7]. In our

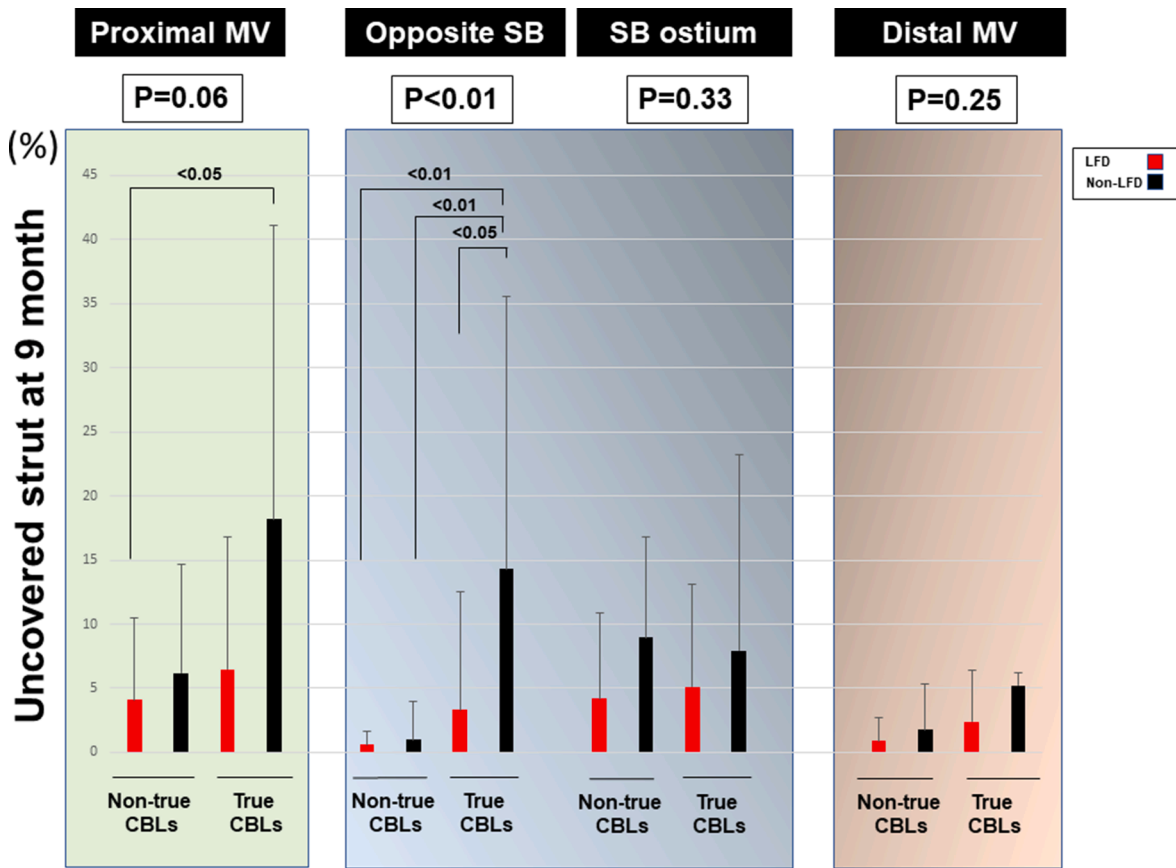


Fig. 7. Uncovered strut at 9 months in proximal MV (light green box on left), opposite SB and SB ostium (light gray box in center), and distal MV (beige box on right) by true CBLs. Red bars indicate LFD group, and black bars display non-LFD group. Same abbreviations are used as Fig. 2. (For interpretation of the references to colour in this figure legend, the reader is referred to the web version of this article.)

study, the average SEI tended to be higher in non-LFD in the distal MV, however, NUS was greater. We speculated that the higher incidence of ISA immediately after KBT in distal MV was more likely to contribute to uneven neointimal proliferation than stent asymmetry expansion. In addition, ISA remained after 9 months at the SB ostium, leading to local flow disturbance and uneven neointimal proliferation in the distal MV. A previous virtual simulation study on CBLs-PCI comparing proximal (sub-optimal) and distal (optimal) re-wiring demonstrated that proximal re-wiring was associated with the formation of longer new metallic carina after strut-opening, which induced a wider area of low WSS and recirculation at both the new carina and lateral walls including proximal SB and distal MV [19]. These hemodynamic changes could influence drug deposition, cause uneven arterial healing post stenting, and result in local fibrin and platelet deposition [9,19]. A recent randomized PROPOT trial, which compared conventional KBT and POT followed by SB angioplasty in provisional bifurcation stenting, showed no significant impact of POT on the rate of strut malapposition in the bifurcation or on the rate of SB-jailing struts [5]. Insufficient stent expansion in the bifurcation core after POT was associated with bifurcation stent failure, including significant strut malapposition, and remaining SB-jailing struts which was related to unfavorable vascular healing [14]. Appropriate positioning of the POT balloon at the carina with an optimal size

for proximal MV defined under imaging guidance is crucial for sufficient stent expansion in the bifurcation core [14].

Immediately after stenting, the MSA is likely to be found in the distal segment of the stent; however, it has been well-expanded in cases of greater vessel tapering including significant SB [20]. In our study, lesions with MSA < 4.5 mm² were more frequently observed in the distal MV than in the proximal MV. However, there was no occurrence of TLR in these small MSA (<4.5 mm²) segments during the 9-month follow-up.

Recently, Nakamura D et al. reported that a new OCT-derived volumetric minimum expansion index (MEI) was a strong predictor of 1-year clinical outcome [20]. The MEI was determined, considering vessel tapering and the presence of major SBs, resulting in an ideal lumen profile that tapers from the proximal to the distal part [20]. Importantly, the authors reported that MEI location differed from MSA post-stent in almost 50% of cases [20]. In general, the proximal MV is considered a potentially larger vessel with more likelihood for accumulated plaque than the distal MV [21]. Previous randomized trials showed that the occurrence of restenosis was more likely clustered in the proximal MV in provisional single stenting with KBT [22].

Final POT could optimize a stent under-expansion in the proximal MV, which might not be displayed as MSA. Furthermore, this technique is a valuable option for correcting ISA and inadequate strut embedment

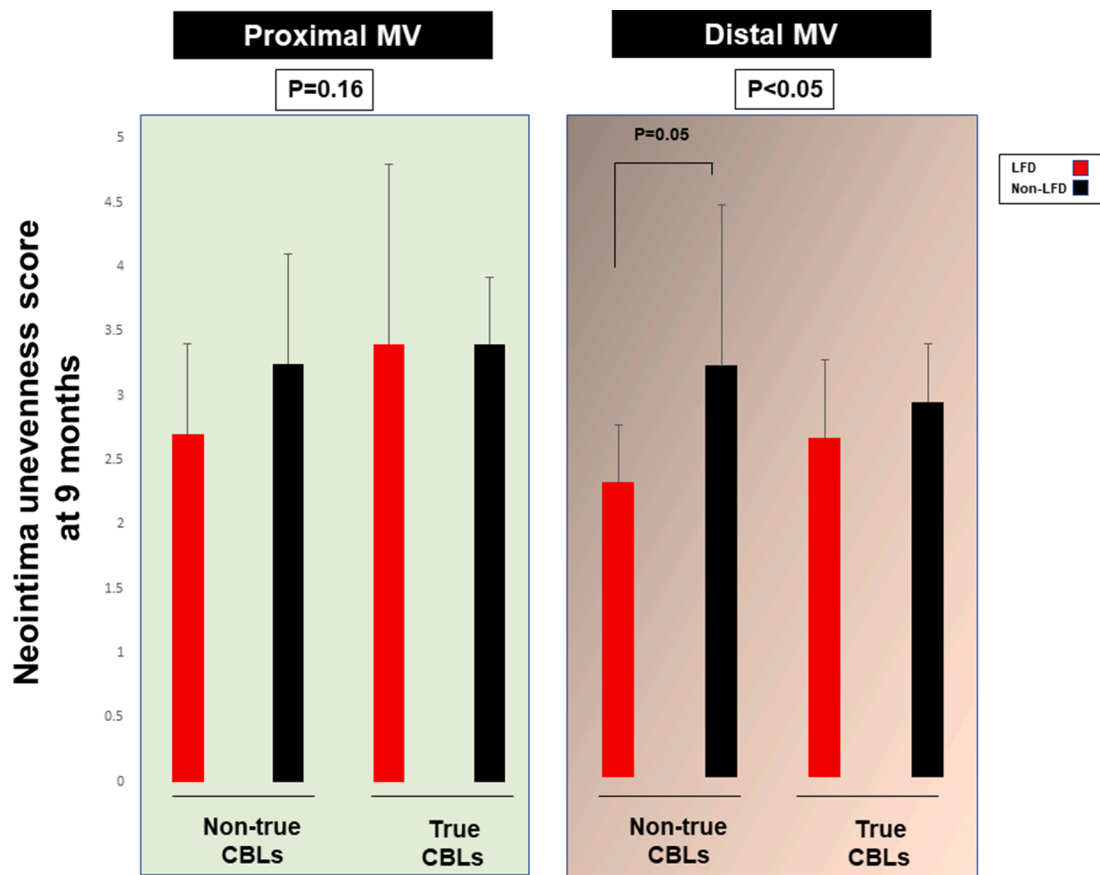


Fig. 8. Neointima unevenness score at 9 months in proximal MV (light green box on left), SB (light gray box in center), and distal MV (beige box on right) by true CBLs. Red bars indicate LFD group, and black bars display non-LFD group. Same abbreviations are used as Fig. 2. NUS was not analyzed due to lack of SB strut opened by KBT in bifurcation core segment. (For interpretation of the references to colour in this figure legend, the reader is referred to the web version of this article.)

Table 4
Nine-month clinical outcome, angiographic restenosis and diameter stenosis on QCA.

	LFD (n = 35)	Non-LFD (n = 24)	p-value
Major adverse cardiovascular events	2 (6)	1 (4)	0.68
Cardiac death	1 (3)	0 (0)	0.40
Myocardial infarction	1 (3)	0 (0)	0.40
Target lesion revascularization	2 (6)	1 (4)	0.68
Stent thrombosis	1 (3)	0 (0)	0.40
Restenosis			
Proximal main vessel	1 (3)	0 (0)	0.40
Distal main vessel	1 (3)	0 (0)	0.40
Side branch	2 (6)	6 (25)	0.08
QCA			
Proximal main vessel, %DS	8.1 ± 7.3	5.3 ± 6.5	0.14
Distal main vessel, %DS	12.4 ± 10.1	15.4 ± 9.1	0.26
Side branch, %DS	25.0 ± 13.4	26.6 ± 17.6	0.72

LFD = link-free on carina and distal guidewire recrossing, QCA = quantitative coronary angiography, %DS = percent diameter stenosis.

induced by strut deformation due to KBT in the non-LFD condition.

5. Conclusions

In provisional CBL stenting followed by KBT, suboptimal SB wiring and significant ISA at the SB orifice increased likelihood of uncovered struts and restenosis at SB orifice, and uneven neointima proliferation in distal MV at 9-month follow-up period. Visualization of the wire recrossing point and the SB-jailing strut pattern by OCT plays an important role to optimize the KBT in CBL stenting, resulting in favorable mid-term vascular healing.

6. Limitations

Post-hoc 3D-OCT analysis was performed in the core laboratory after the procedure. The number of patients undergoing 9-months follow up OCT was small, not randomized, and lacked statistical power for clinical outcomes. In addition, reduced use of POT might affect the rate of distal wiring, because POT facilitates distal wiring and improves proximal apposition. POT was not globally practiced in Japan during the study period. Various types of DESs were used in this registry. Further studies including a larger number of randomized patients and long-term follow-up are required to elucidate the clinical outcome and impact of OCT-guided PCI for CBLs.

Table 5

Sub-analysis between LFD and non-LFD groups on %DS before, immediately after, and 9 months after PCI by the presence or absence of true CBLs.

	Non-true CBLs		True CBLs		p-value
	LFD (n = 16)	Non-LFD (n = 18)	LFD (n = 16)	Non-LFD (n = 5)	
Proximal MV					
Before, %	26.6 ± 23.1	20.3 ± 26.2	35.8 ± 24.5	30.1 ± 34.4	0.37
After, %	7.4 ± 7.7	4.2 ± 6.2	10.0 ± 10.6	2.9 ± 4.4	0.14
9-months, %	5.9 ± 5.3	5.7 ± 7.0	10.3 ± 8.5	3.4 ± 4.1	0.13
Distal MV					
Before, %	46.5 ± 19.7	51.1 ± 19.7	36.5 ± 18.7	41.3 ± 29.7	0.22
After, %	11.8 ± 9.5	15.4 ± 11.0	9.7 ± 8.2	8.3 ± 4.1	0.27
9-months, %	11.3 ± 8.8	13.2 ± 8.2	13.5 ± 11.4	23.1 ± 8.8	0.12
SB					
Before, %	18.1 ± 19.3	21.7 ± 17.8	38.7 ± 21.3	39.2 ± 15.6	<0.01
After, %	17.4 ± 13.5	26.4 ± 16.0	24.6 ± 14.7	42.4 ± 16.7	0.02
9-months, %	22.3 ± 10.2	21.7 ± 9.4	27.7 ± 16.0	43.7 ± 29.0	0.02

CBLs = coronary bifurcation lesions, MV = main vessel, SB = side branch, %DS = diameter stenosis analyzed in Corelab, true bifurcation is defined as CBLs having lesions (%DS > 50% in visual estimates from each center) in both MV and SB such as Medina (1.1.1), (0.1.1), and (1.0.1).

Declaration of Competing Interest

The authors declare that they have no known competing financial interests or personal relationships that could have appeared to influence the work reported in this paper.

Acknowledgement

This study was supported by an unrestricted research grant from the 3D-OCT bifurcation registry.

Dr. Okamura and Dr. Shite received honoraria for technical consulting from Abbott. The other authors have no conflicts of interest to declare.

References

- J.F. Lassen, N.R. Holm, G. Stankovic, T. Lefèvre, A. Chieffo, D. Hildick-Smith, M. Pan, O. Darremont, R. Albiero, M. Ferenc, Y. Louvard, Percutaneous coronary intervention for coronary bifurcation disease: consensus from the first 10 years of the European Bifurcation Club meetings, *EuroIntervent.: J. EuroPCR Collab. Work. Group Intervent. Cardiol. Eur. Soc. Cardiol.* 10 (5) (2014) 545–560.
- Y. Onuma, N. Kogame, Y. Sotomi, Y. Miyazaki, T. Asano, K. Takahashi, H. Kawashima, M. Ono, Y. Katagiri, H. Kyono, S. Nakatani, T. Muramatsu, F. Sharif, Y. Ozaki, P.W. Serruys, T. Okamura, A Randomized Trial Evaluating Online 3-Dimensional Optical Frequency Domain Imaging-Guided Percutaneous Coronary Intervention in Bifurcation Lesions, *Circulat. Cardiovasc. Intervent.* 13 (12) (2020), <https://doi.org/10.1161/CIRCINTERVENTIONS.120.009183>.
- A.P. Banning, J.F. Lassen, F. Burzotta, T. Lefèvre, O. Darremont, D. Hildick-Smith, Y. Louvard, G. Stankovic, Percutaneous coronary intervention for obstructive bifurcation lesions: the 14th consensus document from the European Bifurcation Club, *EuroIntervent.: J. EuroPCR Collab. Work. Group Intervent. Cardiol. Eur. Soc. Cardiol.* 15 (1) (2019) 90–98.
- F.J. Neumann, M. Sousa-Uva, A. Ahlsson, et al., 2018 ESC/EACTS Guidelines on myocardial revascularization, *Eur. Heart J.* 40 (2019) 87–165.
- Y. Watanabe, Y. Murasato, M. Yamawaki, Y. Kinoshita, M. Okubo, K. Yumoto, N. Masuda, H. Otake, J. Aoki, G. Nakazawa, Y. Numasawa, T. Ito, J. Shite, T. Okamura, K. Takagi, K. Kozuma, T. Lefèvre, B. Chevalier, Y. Louvard, N. Suzuki, K. Kozuma, Proximal optimisation technique versus final kissing balloon inflation in coronary bifurcation lesions: the randomised, multicentre PROPOT trial, *EuroIntervent.: J. EuroPCR Collab. Work. Group Intervent. Cardiol. Eur. Soc. Cardiol.* 17 (9) (2021) 747–756.
- T. Okamura, R. Nagoshi, T. Fujimura, Y. Murasato, M. Yamawaki, S. Ono, T. Serikawa, Y. Hikichi, H. Norita, F. Nakao, T. Sakamoto, T. Shinke, J. Shite, Impact of guidewire recrossing point into stent jailed side branch for optimal kissing balloon dilatation: core lab 3D optical coherence tomography analysis, *EuroIntervent.: J. EuroPCR Collab. Work. Group Intervent. Cardiol. Eur. Soc. Cardiol.* 13 (15) (2018) e1785–e1793.
- H. Otake, J. Shite, J. Aoki, T. Shinke, Y. Tanino, D. Ogasawara, T. Sawada, N. Miyoshi, H. Kato, B.-K. Koo, Y. Honda, P.J. Fitzgerald, K.-I. Hirata, Local determinants of thrombus formation following sirolimus-eluting stent implantation assessed by optical coherence tomography, *JACC Cardiovasc. Intervent.* 2 (5) (2009) 459–466.
- D. Terashita, H. Otake, T. Shinke, Y. Murasato, Y. Kinoshita, M. Yamawaki, Y. Takeda, K. Fujii, S.-I. Yamada, Y. Shimada, T. Yamashita, K. Yumoto, K.-I. Hirata, Differences in Vessel Healing Between Sirolimus- and Everolimus-Eluting Stent Implantation for Bifurcation Lesions: The J-REVERSE Optical Coherence Tomography Substudy, *Can. J. Cardiol.* 32 (3) (2016) 384–390.
- W.S. Nesbitt, P. Mangin, H.H. Salem, S.P. Jackson, S. Stavnes, T.K. Steigen, The impact of blood rheology on the molecular and cellular events underlying arterial thrombosis, *J. Mole. Med. (Berlin, Germany)* 84 (12) (2006) 989–995.
- H. Hariki, T. Shinke, H. Otake, J. Shite, M. Nakagawa, T. Inoue, T. Osue, M. Iwasaki, Y.u. Taniguchi, R. Nishio, N. Hiranuma, H. Kinutani, A. Konishi, K.-I. Hirata, Potential benefit of final kissing balloon inflation after single stenting for the treatment of bifurcation lesions—insights from optical coherence tomography observations, *Circul. J.: Offic. J. Jpn. Circul. Soc.* 77 (5) (2013) 1193–1201.
- M. Niemelä, K. Kervinen, A. Erglis, N.R. Holm, M. Maeng, E.H. Christiansen, I. Kumsars, S. Jegere, A. Dombrovskis, P. Gunnæs, S. Stavnes, T.K. Steigen, T. Trovik, M. Eskola, S. Vikman, H. Romppanen, T. Mäkkikallio, K.N. Hansen, P. Thayssen, L. Aberg, L.O. Jensen, A. Hervold, J. Airaksinen, M. Pietilä, O. Probert, T. Kellerth, J. Ravkilde, J. Aarøe, J.S. Jensen, S. Helqvist, I. Sjögren, S. James, H. Miettinen, J.F. Lassen, L. Thuesen, Randomized comparison of final kissing balloon dilatation versus no final kissing balloon dilatation in patients with coronary bifurcation lesions treated with main vessel stenting: the Nordic-Baltic Bifurcation Study III, *Circulation* 123 (1) (2011) 79–86.
- C.W. Yu, J.H. Yang, Y.B. Song, et al., Long-Term Clinical Outcomes of Final Kissing Ballooning in Coronary Bifurcation Lesions Treated With the 1-Stent Technique: Results From the COBIS II Registry (Korean Coronary Bifurcation Stenting Registry), *JACC Cardiovasc. Intervent.* 8 (2015) 1297–1307.
- Y. Murasato, T. Mori, T. Okamura, R. Nagoshi, T. Fujimura, M. Yamawaki, S. Ono, T. Serikawa, F. Nakao, J. Shite, Efficacy of the proximal optimization technique on crossover stenting in coronary bifurcation lesions in the 3D-OCT bifurcation registry, *Int. J. Cardiovasc. Imag.* 35 (6) (2019) 981–990.
- Y. Murasato, Y. Watanabe, M. Yamawaki, et al., Effect of proximal optimization technique on coronary bifurcation stent failure: Insights from the multicenter randomized PROPOT trial, *Cathet. Cardiovasc. Intervent.: Offic. J. Soc. Cardiac Angiogr. Intervent.* (2022).
- Y. Onuma, Y. Katagiri, F. Burzotta, N.R. Holm, N. Amabile, T. Okamura, G.S. Mintz, O. Darremont, J.F. Lassen, T. Lefèvre, Y. Louvard, G. Stankovic, P.W. Serruys, Joint consensus on the use of OCT in coronary bifurcation lesions by the European and Japanese bifurcation clubs, *EuroIntervent.: J. EuroPCR Collab. Work. Group Intervent. Cardiol. Eur. Soc. Cardiol.* 14 (15) (2019) e1568–e1577.
- R. Nagoshi, T. Okamura, J. Shite, A Novel Push-Fold Method for Removing Side Branch-Jailed Stent Struts Under 3D Optical Coherence Tomography Guidance, *JACC Cardiovasc. Intervent.* 9 (11) (2016) e107–e109.
- N.R. Holm, L.N. Andreasen, S. Walsh, O.A. Kajander, N. Witt, C. Eek, P. Knaapen, L. Koltowski, J.L. Gutiérrez-Chico, F. Burzotta, J. Kockman, J. Ormiston, I. Santos-Pardo, P. Laanmets, D. Mylotte, M. Madsen, J. Hjort, I. Kumsars, T. Råmunddal, E. H. Christiansen, Rational and design of the European randomized Optical Coherence Tomography Optimized Bifurcation Event Reduction Trial (OCTOBER), *Am. Heart J.* 205 (2018) 97–109.
- M. Watanabe, S. Uemura, Y. Kita, Y.u. Sugawara, Y. Goryo, T. Ueda, T. Soeda, S. Okayama, H. Okura, T. Kume, Y. Saito, Impact of branching angle on neointimal coverage of drug-eluting stents implanted in bifurcation lesions, *Coron. Artery Dis.* 27 (8) (2016) 682–689.
- S. Morlacchi, C. Chiastra, E. Cutri, P. Zunino, F. Burzotta, L. Formaggia, G. Dubini, F. Migliavacca, Stent deformation, physical stress, and drug elution obtained with provisional stenting, conventional culotte and Tryton-based culotte to treat bifurcations: a virtual simulation study, *EuroIntervent.: J. EuroPCR Collab. Work. Group Intervent. Cardiol. Eur. Soc. Cardiol.* 9 (12) (2014) 1441–1453.

- [20] D. Nakamura, W. Wijns, M.J. Price, M.R. Jones, E. Barbato, T. Akasaka, S.-L. Lee, S. M. Patel, S. Nishino, W. Wang, A. Gopinath, G.F. Attizzani, D. Holmes, H. G. Bezerra, New Volumetric Analysis Method for Stent Expansion and its Correlation With Final Fractional Flow Reserve and Clinical Outcome: An ILUMIEN I Substudy, *JACC Cardiovasc. Intervent.* 11 (15) (2018) 1467–1478.
- [21] O. Badak, P. Schoenhagen, T. Tsunoda, W.A. Magyar, J. Coughlin, S. Kapadia, S. E. Nissen, M.E. Tuzcu, Characteristics of atherosclerotic plaque distribution in coronary artery bifurcations: an intravascular ultrasound analysis, *Coron. Artery Dis.* 14 (4) (2003) 309–316.
- [22] Y.-H. Kim, J.-H. Lee, J.-H. Roh, J.-M. Ahn, S.-H. Yoon, D.-W. Park, J.-Y. Lee, S.-C. Yun, S.-J. Kang, S.-W. Lee, C.W. Lee, K.B. Seung, W.-Y. Shin, N.-H. Lee, B.-K. Lee, S.-G. Lee, C.-W. Nam, J. Yoon, J.-Y. Yang, M.-S. Hyon, K. Lee, J.-S. Jang, H.-S. Kim, S.-W. Park, S.-J. Park, Randomized Comparisons Between Different Stenting Approaches for Bifurcation Coronary Lesions With or Without Side Branch Stenosis, *JACC Cardiovasc. Intervent.* 8 (4) (2015) 550–560.